Proceedings World Geothermal Congress 2010
Bali, Indonesia, 25-29 April 2010

Three Dimensional Numerical Modeling of Fracture Flow for Rock Core Coupled with X-Ray Computed Tomography

Noriaki Watanabe[*1], Yutaka Ohsaki[2], Tetsuya Tamagawa[2], Nobuo Hirano[1], Yoshihiro Tsuchiya[3], Hiroshi Okabe[3], and Noriyoshi Tsuchiya[1]

[1]Graduate School of Environmental Studies, Tohoku University, 6-6-20 Aoba, Aramaki, Aoba-ku, Sendai 980-8597 Japan

[2]JAPEX Research Center, Japan Petroleum Exploration Co., Ltd., 1-2-1 Hamada, Mihama-ku, Chiba 261-0025 Japan

[3]EOR Research Division, Technology Research & Development Department, JOGMEC, 1-2-2 Hamada, Mihama-ku, Chiba 261-0025 Japan

[*]watanabe@mail.kankyo.tohoku.ac.jp

Keywords: three dimensional numerical modeling, fracture flow, rock core, X-ray computed tomography

ABSTRACT

A three dimensional numerical modeling coupled with X-ray Computed Tomography (CT) for fracture flow was applied to fractured granite core samples. One of the samples had an artificial single fracture, and the others had natural multiple fractures. A relationship between CT value and fracture aperture (fracture aperture calibration curve) was first obtained by X-ray CT scanning for a fracture calibration standard with varying fracture apertures (0.1-0.5 mm). As a result, a linear relationship was obtained. With the fracture aperture calibration curve, three dimensional distributions of CT values of the samples were converted into fracture aperture distributions to obtain fracture models of the samples. Porosities of the fracture models could provide good agreement with experimentally determined porosities for all the samples. By using the fracture models, a fluid flow simulation was also performed with a local cubic law-based fracture flow model. Numerical permeabilities by the flow simulation were much higher than experimentally determined permeabilities of the samples. It was however possible to match the numerical permeabilities with the experimental permeabilities for all samples, by using a unique modification coefficient of 0.5 for the fracture aperture in the fracture flow model. Although the X-ray CT scanning was performed at room temperature and pressure, it was expected that the numerical modeling had the possibility to provide insights into the heterogeneous nature of fracture flow, such as channeling in reservoirs, as well as porosity and permeability.

1. INTRODUCTION

For effective development of natural geothermal reservoirs and the Enhanced Geothermal Systems (EGSs), it is essential to understand fracture flow characteristics in the reservoirs. Field and laboratory studies have suggested that fluid flow through a rock fracture is very different from fluid flow through smooth parallel plates, due to channeling flow in a heterogeneous aperture distribution by rough surfaces (Cacas et al., 1990; Abelin et al., 1991; Dverstorp et al., 1992; Carmeliet et al., 2004; Johnson et al., 2006; Rowland et al., 2008; Watanabe et al., 2008l Nemoto et al., 2009; Watanabe et al., 2009). When channeling flow occurs in a single fracture of granite, the area where flowing fluid exists is expected at only 5-20% at confining pressures of up to 100 MPa, with various features in the preferential flow paths (Watanabe et al, 2009). It is suggested that channeling flow should be evaluated to understand the reality of fracture flow in a reservoir.

Because the aperture distribution can be affected by fracturing processes, stress conditions, water-rock interactions, and so on, a fracture flow analysis for a fractured rock core by the drilling is the most effective way to obtain insights into the heterogeneous fracture flow of the reservoir. However, naturally fractured rock cores, which often contain multiple fractures, are usually much more difficult to evaluate in terms of channeling flow. Although fracture flow analyses by numerical fracture models with heterogeneous aperture distributions are effective (Watanabe et al., 2008; Nemoto et al., 2008; Watanabe et al., 2009), a precise aperture determination is much more challenging for multiple fractures with existing methods. Because available rock cores of a reservoir are limited, it is required to develop a practical numerical modeling that is coupled with a non-destructive precise aperture determination.

X-ray Computed Tomography (CT) has been one of the most effective non-destructive methods to analyze internal structures such as fractures in rocks, sometimes with fluid flow within them (Keller et al., 1995; Pylak-Nolte et al., 1997; Johns et al., 1993; Coles et al., 1998; Keller, 1998; Keller et al., 1999; Montemagno and Pyrak-Nolte, 1999; Scavia, 1999; Bertels et al., 2001; Richard et al., 2001; Rangel-German and Kovscek, 2002; Hirono et al., 2003; Polak et al., 2003; Polak et al., 2004; Hirono, 2005; Cnudde et al., 2006; Liu et al., 2006; Yasuhara et al., 2006; Rebeiro et al., 2007; Zhu et al., 2007; David et al., 2008; Nakashima et al., 2008). In addition, previous studies have already shown the possibility of precise fracture aperture determination by using X-ray CT, sometimes with a fracture flow simulation with the apertures (Johns et al., 1993; Keller et al., 1995; Pylak-Nolte et al., 1997; Keller, 1998; Keller et al., 1999; Montemagno and Pyrak-Nolte, 1999; Bertels et al., 2001). Consequently, a numerical fracture flow analysis with an aperture distribution by X-ray CT is one of the most favorable options for rock cores. However, the relevance of such kind of methods in previous studies had been unclear due to lack of quantitative evaluation of numerical results in light of independent experimental results, such as porosities and/or permeabilities. In addition, results for multiple fractures were very few.

In the present study, we therefore focused on the feasibility of a precise three dimensional numerical modeling of fracture flow coupled with X-ray CT for a rock core to provide insights into heterogeneous nature of fracture flow,

such as channeling flow, in reservoirs. A third generation X-ray CT scanner, which provided relatively high voxel resolution of less than 1 mm^3, was used for precise imaging of fractured granite core samples with an artificial single fracture or natural multiple fractures. Fracture models (i.e. aperture distributions) obtained by the CT images were evaluated by comparison of numerically and experimentally determined porosities of the samples. In addition, a fluid flow simulation was performed for the fracture models using a local-cubic law based fracture flow model. The fracture flow model was also evaluated by using the experimentally determined permeabilities of the samples.

2. METHODS

2.1 X-ray Computed Tomography

2.1.1 Fracture Aperture Calibration

To develop three dimensional models of fractured rock cores, it is needed to convert CT images of the rock cores into three dimensional fracture aperture distributions within them, using a fracture aperture calibration curve (Johns et al., 1993; Keller, 1998; Bertels et al., 2001). Therefore, we first scanned a fracture aperture calibration standard with known fracture apertures to prepare the calibration curve. We then scanned fractured rock core samples to obtain input data for the modeling.

The X-ray CT scanning was performed at the Japan Oil, Gas, and Metals National Corporation Technology and Research Center (JOGMEC TRC), with the Aquilion™ third generation scanner produced by Toshiba Medical Systems Corporation (Figure 1). The CT scanner provides a three dimensional distribution of CT values (a measure of X-ray attenuation), with a voxel resolution of 0.35 x 0.35 x 0.50 mm^3, within several minutes for the sample dimensions used in the present study. The parametric values of the CT scanner are summarized in Table 1. The parametric values were constant throughout all CT scans in the present study.

Figure 1: The third generation X-ray CT scanner, the Aquilion™, of the JOGMEC TRC.

The CT values at each voxel depend on densities of the materials. With increasing density, the CT values also increase. Because of this fundamental principle, we can detect the presence of a fracture as apparent density reduction, compared with the original density of the material, even if the fracture is smaller than the voxel. The apparent density reduction depends on the pore volume, which in turn depends on fracture aperture. Consequently, we can convert CT values into fracture aperture when a relationship between CT value and fracture aperture (a fracture aperture calibration curve) is obtained.

Table 1: The parameter values of the X-ray CT scanner, the Aquilion™, of the JOGMEC TRC.

Parameter	Value
Voltage	120 kV
Current	150 mA
Slice thikness	0.50 mm
Pixcel resolution of the slice	0.35 mm
Pixcel matrix size	512 x 512

The aperture calibration standard with known fracture apertures were a cylindrical granite having a simulated single fracture with an unique aperture. The fracture was prepared by cutting a granite of 100 mm in diameter and 45 mm in length. The fracture surfaces were polished, and finally had a mean roughness of ca. 20-30 μm. The aperture was created by inserting a thickness gauge within the fracture. The calibration standard was scanned with varying aperture (0.1-0.5 mm) by changing the thickness of the gauge.

2.1.2 Imaging Fractured Granite Cores

It is important to develop a three dimensional numerical modeling not only for a single fracture but also for multiple fractures, because rock cores by the drilling usually contain multiple fractures. We therefore used fractured granite cores, which contained a single fracture or multiple fractures, with known porosities and permeabilities for evaluation of relevance of the modeling.

Three fractured granite core samples were scanned with the X-ray CT scanner described above, with the same parameter values. One of the samples contained a single fracture, and the others contained multiple fractures. The sample with a single fracture (Sample 1) was cylindrical granite with a tensile fracture generated in a laboratory by using a wedge. The samples with multiple fractures (samples 2 and 3) were naturally fractured granite cores from granite bedrock at a depth of ca. 4500-4600 m in Japan. The diameters (ϕ) and lengths (l) of the samples were 100 mm (ϕ) x 150 mm (l) for the sample 1, and 100 mm (ϕ) x 120 mm (l) for the samples 2 and 3.

2.2 Three Dimensional Numerical Modeling

2.2.1 Fracture Modeling

Once a fracture calibration curve is obtained, we can convert CT values at each voxel into fracture apertures, providing three dimensional fracture models of the samples. In addition, we can simulate fluid flow through the fracture models by utilizing existing fracture flow models for a variable fracture aperture. Because porosities and permeabilities can be calculated for the models, comparisons of calculated values with experimental values provide quantitative evaluations of the models.

In the fracture modeling, we assumed a smooth parallel plate single fracture with a unique aperture and orientation for each voxel (Figure 2), although the voxels might contain multiple fractures with various apertures and orientations in reality. This is the same relationship between fracture and voxel in the determination of the fracture aperture calibration curve. Therefore, the CT values of the samples were directly converted into fracture apertures with the aperture calibration curve. Note that the maximum fracture aperture was Δy in Figure 2. In addition, porosity of a

fracture model was calculated by integrating fracture volumes of all voxels.

2.2.2 Fracture Flow Modeling

For modeling fracture flow in three dimensions (*x*-*y*-*z* coordinates), we employed a Local Cubic Law (LCL)-based fracture flow model for laminar flow of a viscous fluid at steady state. With a constant viscosity, the equation of continuity for Darcy's flow can be described as (Brown, 1987; Mourzenko et al., 1995; Zimmerman and Bodvarsson, 1996; Ge, 1997; Oron and Berkowitz, 1998; Yeo et al., 1998; Pyrak-Nolte and Morris, 2000; Brush and Thomson, 2003; Konzuk and Kueper, 2004; Watanabe et al., 2008; Nemoto et al., 2009; Watanabe et al., 2009):

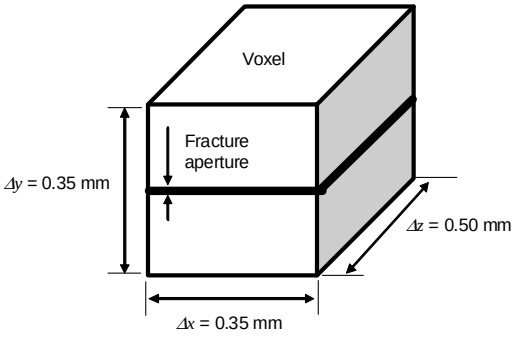

Figure 2: The smooth parallel plate fracture for the voxel of 0.35 x 0.35 x 0.50 mm^3 in the fracture modeling.

$$\frac{\partial}{\partial x}\left(Ak\frac{\partial P}{\partial x}\right)+\frac{\partial}{\partial y}\left(Ak\frac{\partial P}{\partial y}\right)+\frac{\partial}{\partial z}\left(Ak\frac{\partial P}{\partial z}\right)=0 \quad (1)$$

where A is the cross-sectional area where fluid flows, k is the permeability, and P is the fluid pressure. In the LCL, A and k in the equation (1) are described as:

$$A = wa \quad (2)$$

$$k = \frac{a^2}{12} \quad (3)$$

where w and a are the width and the aperture of the fracture. In the present study, w was assumed to be Δx in Figure 2 (no significant difference between Δx and Δz), and the product Ak was assumed to be isotropic at a voxel although the fracture has a specific orientation in the fracture modeling. Note that A was the area of the voxel-voxel interface without the modification, and k was constant (rock matrix permeability: 10^{-20} m^2), for voxels with zero-fracture aperture.

By solving the finite difference form of the equation (1) at given boundary conditions, we determined flow rate distributions and permeabilities for fracture models. Because permeability measurements of the samples had been performed with unidirectional flow in the axial direction, the boundary conditions were given so that the same flow geometry was achieved.

3. RESULTS AND DISCUSSION

3.1 Fracture Aperture Calibration Curve

In the X-ray CT scanning for the fracture aperture calibration standard, fracture signals were observed as relatively large drops of the CT values (Figure 3). However, it was difficult to find the fracture signal for the fracture aperture of 0.1 mm due to variation of CT value for the rock matrix. The CT value for such small fracture aperture could therefore have some uncertainty. The variation could be caused by the presence of rock-forming minerals with different densities, as described later. Note that the elevated CT values near the sample edges were responsible for the beam hardening (Ketcham and Carlson, 2001).

The relationship between CT values and fracture aperture was linear (Figure 4), and was well fitted by the least squares method with the following equation:

$$ct = -2222a + 1689 \quad (4)$$

where ct is the CT value, and a is the fracture aperture. The relatively large deviation of the CT value from the regression curve at the fracture aperture of 0.1 mm may have been caused by the uncertainty mentioned above. The CT value at the intercept (a = 0) was 1689. This value was quite similar to the mean CT value of granite in Keller (1998). Despite the uncertainty, it was concluded that the fracture aperture calibration curve was reasonable.

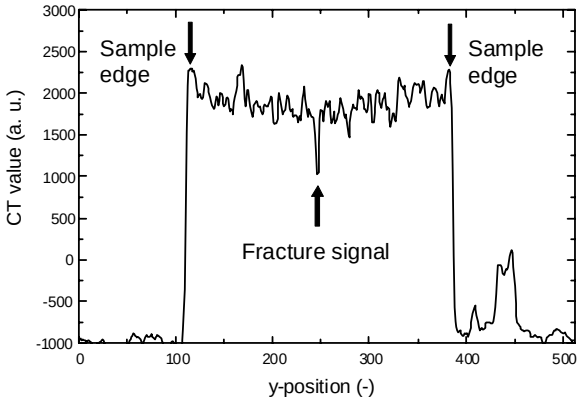

Figure 3: An example of the fracture signal obtained by the X-ray CT scanning for the facture aperture calibration standard.

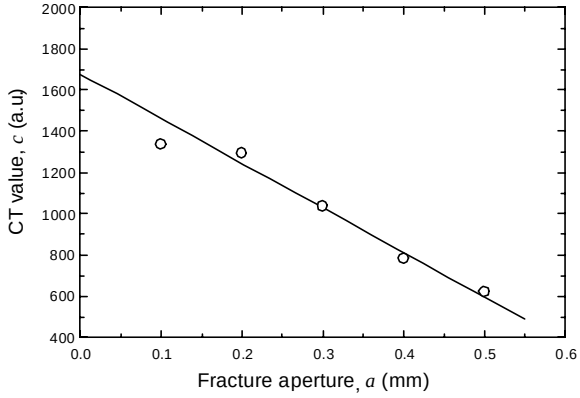

Figure 4: The relationship between CT value and fracture aperture by the X-ray CT scanning for the fracture aperture calibration standards. The solid line is the linear regression curve by the least squares method.

3.2 CT Images of Fractured Granite Core Samples

As described above, the CT images of the samples also have varying CT values for the rock matrix and elevated values at sample edges (Figures 5-7). A wide range

variation of CT values was observed, corresponding to light grey regions, where CT values were ca. 1600-2500. This variation could be responsible for the rock-forming minerals with different densities, because the shape and distribution seemed similar to those of minerals. However, the aperture calibration curves with the CT value of 1689 at zero-fracture aperture suggested that this variation had less significant effects in the aperture determination, because most CT values in the variation were greater than 1689, and were all recognized as the rock matrix.

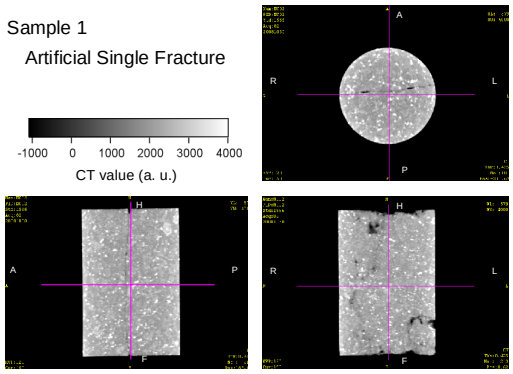

Figure 5: The CT images of sample 1 containing an artificial single fracture.

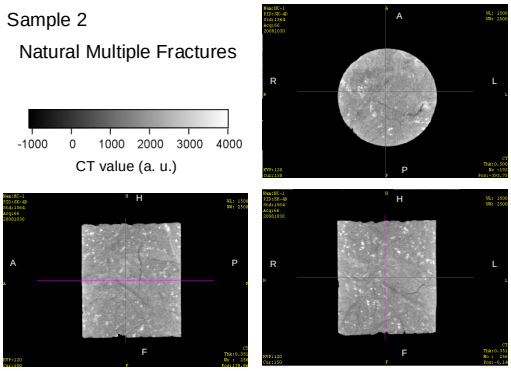

Figure 6: The CT image of the sample 2 containing multiple natural fractures.

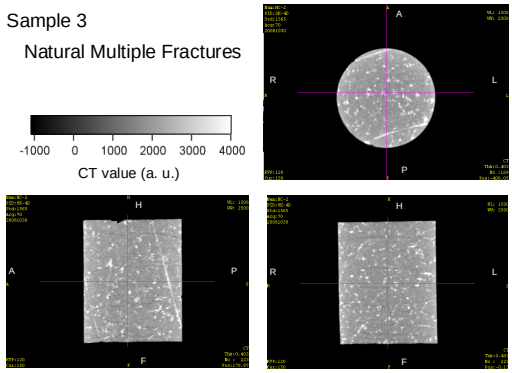

Figure 7: The CT image of the sample 3 containing multiple natural fractures.

3.3 Fracture Models

With the fracture aperture calibration curve described by equation (4), the fracture modeling was performed for the fractured granite core samples. In the modeling, CT values near the sample edges were not used due to the elevated CT values caused by the beam hardening as described above. Consequently, the models of the samples were not cylindrical, but rectangular with the dimensions of 60 x 60 x 150 mm^3 for the sample 1, and 60 x 60 x 120 mm^3 for the samples 2 and 3.

The numerical porosities of the samples were 1.2%, 4.5%, and 2.3% for samples 1, 2, and 3, respectively. Because the X-ray CT scanning was performed at standard pressure, the numerical results corresponded to the samples at that condition. Although we had porosities of the samples, the results were obtained at confining pressures of < 35 MPa. We therefore compared the numerical porosities with the values inferred by extrapolation of the experimental results (Figure 8). The numerical porosities were very close to the inferred porosities of the samples at standard pressure. The discrepancies of the porosities were within ca. 1%. The discrepancy was greater for the samples with greater porosity and multiple fractures (samples 2 and 3). Although the reason for the discrepancies is not clear, it may be very difficult to obtain much better results because some uncertainty of the aperture calibration curve inevitably arises due to fluctuations of CT values caused by rock-forming minerals with different densities. Assuming that the porosities were not significantly different between the original entire volume and the present partial volume of the samples, it was concluded that the present fracture modeling was relevant.

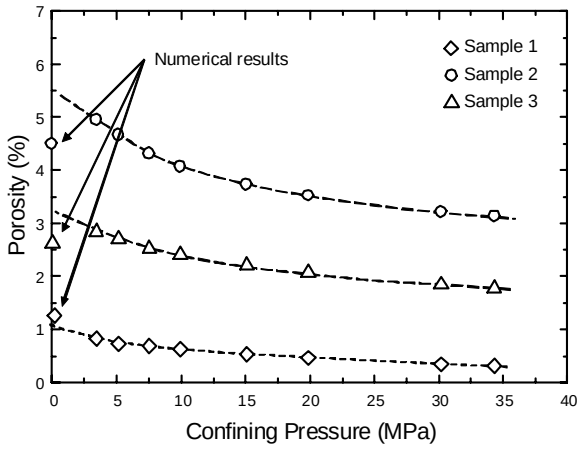

Figure 8: The comparison of the experimental and the numerical porosities of the samples. The experimental porosities had been measured at confining pressures of < 35 MPa, and were utilized to infer the porosities at standard pressure (dashed lines), which were compared with the numerical porosities by fracture models of the samples at the standard pressure.

3.4. Fracture Flow Models

With respect to the fracture models, the fracture flow modeling was performed for the fractured granite core samples. Note that up-scaling of the original voxel was performed due to limitations of our workstation computer. The voxel dimension was changed to 0.70 x 0.70 x 1.0 mm^3. Although the workstation had a relatively high performance (CPU: Intel® Xenon® X5482, RAM: 32 GB), it was too difficult to perform the flow simulation with the original voxel resolution.

The numerical permeabilities were 6.1 x 10^{-14} m^2, 3.3 x 10^{-13} m^2, and 9.2 x 10^{-15} m^2 for samples 1, 2, and 3, respectively. Compared to the inferred permeabilities of the samples at the standard pressure, the numerical permeabilities were much greater (Figure 9a). As well as the porosity the discrepancy was greater for the samples

with multiple fractures (sample 2 and 3). Because the flow model assumed fluid flow though the smooth parallel plate fracture, there should be differences from the reality. Nevertheless, the magnitude relation among the numerical permeabilitis was consistent with the experimental results. It was found that the fracture flow modeling of equations (1)-(3) could provide qualitatively reasonable results. In addition, the discrepancy was found to be similar magnitudes among the three samples. This suggested that numerical results could be improved to match the inferred permeabilities by a unique modification coefficient of the fracture aperture in the equations (2) and (3). In fact, the numerical permeabilities were much improved with the modification coefficient of 0.5 (Figure 9b). Assuming the inferred permeabilities were relevant, it was concluded that the present fracture flow model provided quantitatively reasonable results with the modification coefficient of the fracture aperture.

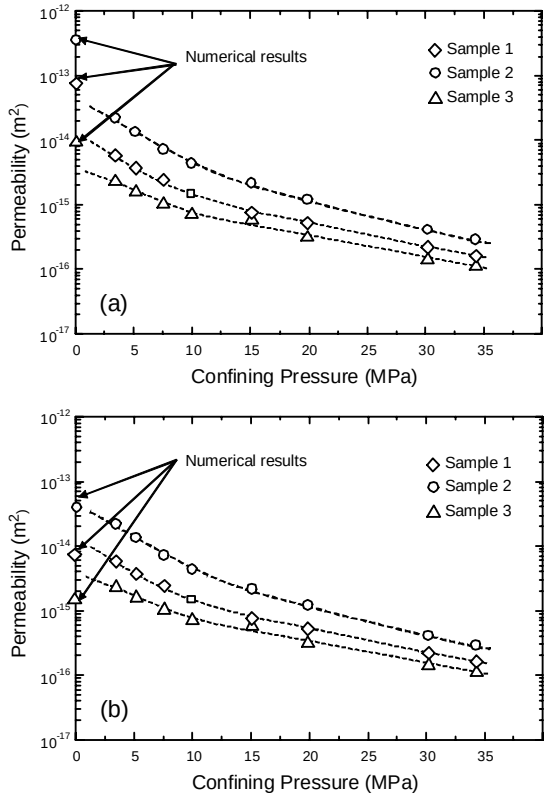

Figure 9: The comparison of the experimental and the numerical permeabilities of the samples. The experimental permebilities were measured at confining pressures of < 35 MPa, and were utilized to predict the permeabilities at standard pressure (dashed lines), which were compared with the numerical permeabilities from the original (a) and the modified (b) fracture flow models of the samples at the standard pressure.

The present models showed that the porosities and the permeabilities of the fractured granite core samples could be predicted even for the natural multiple fractures. Consequently, a precise numerical modeling coupled with X-ray CT was essentially possible, and was a simple effective method to analyze heterogeneous nature of fracture flow such as channeling (Figures 10-12). Although channeling was not so obvious for the present results, probably due to small contact area of fracture surfaces at no confining pressure (Watanabe et al., 2008; Nemoto et al., 2009; Watanabe et al., 2009), the flow paths could be clearly observed particularly for sample 1 with the artificial single fracture. If the X-ray CT scanning is performed at higher temperatures and/or confining pressures (Polak et al., 2003; Polak et al., 2004; Liu et al., 2006; Zhu et al., 2007), the present numerical modeling should provide insights into heterogeneous nature of fracture flow at reservoir conditions.

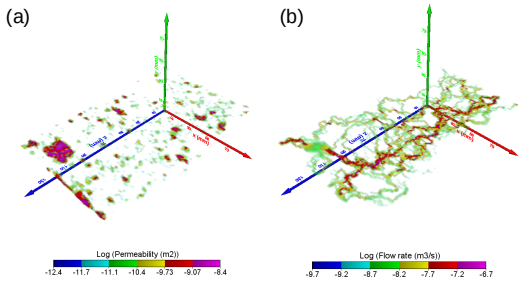

Figure 10: The permeability (a) and flow rate distribution (b) by the numerical modeling of the sample 1, where the flow rate distribution was obtained by the modified fracture flow model. The macroscopic flow direction is parallel to the *z* axis (blue).

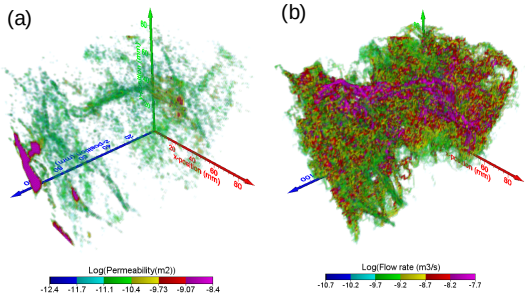

Figure 11: The permeability (a) and flow rate distribution (b) by the numerical modeling of the sample 2, where the flow rate distribution was obtained by the modified fracture flow model. The macroscopic flow direction is parallel to the *z* axis (blue).

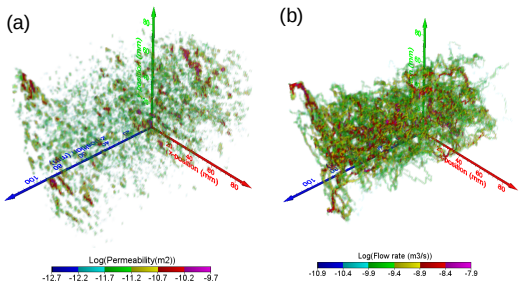

Figure 12: The permeability (a) and flow rate distribution (b) by the numerical modeling of the sample 3, where the flow rate distribution was obtained by the modified fracture flow model. The macroscopic flow direction is parallel to the *z* axis (blue).

4. CONCLUSIONS

Three dimensional numerical molding of fracture flow in rock cores was coupled with X-ray CT and applied to fractured granite core samples having single or multiple fractures. The fracture models obtained with the

relationship between CT value and fracture aperture (fracture aperture calibration curve), resulted in very close values of porosities to those of experimental results. The local cubic law-based fluid flow models led to much greater permeabilities than experimental results when the fracture flow models were directly used in the fluid flow simulation. However, it was possible to match the numerical permeabilities with the experimental results when the modification coefficient of 0.5 was used for fracture apertures in the fracture flow modeling. Consequently, the present numerical modeling could provide quantitatively reasonable results. The numerical modeling should be very useful to obtain insights into heterogeneous nature of fracture flow such as channeling in reservoirs as well as permeability and porosity when X-ray CT scanning is performed at reservoir conditions.

ACKNOWLEDGEMENTS

The authors wish to acknowledge Dr. Kimio Watanabe of RichStone, Ltd. for the coding of the modeling algorithm.

REFERENCES

Abelin, H., Birgersson, L., Moreno, L., Widen, H., Ågren, T., and Neretnieks, I.: A large-scale flow and tracer experiment in granite: 2. Results and interpretation, Water Resour. Res., 27(12), (1991), 3119-3135

Brown, S.R.: Fluid flow through rock joints: The effect of surface roughness, J. Geophys. Res., 92(B2), (1987), 1337-1347

Brush, D.J., and Thomson, N.R.: Fluid flow in synthetic rough-walled fractures: Navier-Stokes, Stokes, and local cubic law assumptions, Water Resour. Res., 39(4), (2003), 1085, doi:10.1029/2002WR001346

Cacas, M.C., Ledoux, E., De Marsily, G., Tillie, B., Barbreau, A., Durand, E., Feuga, B., and Peaudecerf, P.: Modeling fracture flow with a stochastic discrete fracture network: Calibration and validation: 1. The flow model, Water Resour. Res., 26(3), (1990), 479-489

Carmeliet, J., Delerue, J.-F., Vandersteen, K., and Roels, S.: Three-dimensional liquid transport in concrete cracks, Int. J. Numer. Anal. Meth. Geomech., 28, (2004), 671-687, doi:10.1002/nag.373

Ge, S.: A governing equation for fluid flow in rock fractures, Water Resour. Res., 33(1), (1997), 53-61

Cnudde, V.; Masschaele; Dierick, M.; Vlassenbroeck; Van Hoorebeke, L.; Jacobs, P.: Recent progress in X-ray Ct as a geosciences tool, Appl. Geochem., 21, (2006), 826-832

Coles, M.E.; Hazlett, R.D.; Spanne, P.; Soll, W.E.; Muegge, E.L.; Jones, K.W.: Pore level imaging of fluid transport using synchrotron X-ray microtomography, J. Petrol. Sci. Eng., 19, (1998), 55-63

Bertels, S.P., and DiCarlo D.A.: Measurement of aperture distribution, capillary pressure, relative permeability, and in situ saturation in a rock fracture using computed tomography scanning, Water Resour. Res., 37(3), (2001), 649-662

David, C.; Menendez, B.; and Mengus J.-M.: Influence of mechanical damage on fluid flow patterns investigated using CT scanning imaging and acoustic emissons techniques, Geophys. Res. Lett., 35, (2008), L16313, doi: 10.1029/2008GL034879

Dverstorp, B.; Andersson, J.; and Nordqvist, W.: Discrete fracture network interpretation of field tracer migration in sparsely fractured rock, Water Resour. Res., 28(9), (1992), 2327-2343

Hirono, T.: The role of dewatering in the progressive deformation of a sandy accretionary wedge: constraints from direct imaging of fluid flow and void structure, Tectonophys., 397, (2005), 261-280

Hirono, T.; Takahashi, M.; and Nakashima, S.: In situ visualization of fluid flow image within deformed rock by X-ray CT, Eng. Geol., 70, (2003), 37-46

Johnson, J.; Brown, S.; and Stockman H.: Fluid flow and mixing in rough-walled fracture intersections, J. Geophys. Res., 111, (2006), B12206, doi:10.1029/2005JB004087

Johns, R.A.; Steude, J.S.; Castainer, L.M.; and Roberts, P. V.: Nondestructive measurements of fracture aperture in crystalline rock cores using X ray computed tomography, J. Geophys. Res., 98(B2), (1993), 1889-1900

Karpyn, Z.T.; Alajmi, A.; Radaelli, F.; Halleck, P.M.; Grader, A.S.: X-ray CT and hydraulic evidence for a relationship between fracture conductivity and adjacent matrix porosity, Eng. Geol., 103, (2008), 139-145

Keller, A.: High resolution, non-destructive measurement and characterization of fracture apertures, Int. J. Rock Mech. Min. Sci., 35(8), (1998), 1038-1050

Keller, A.A.; Roberts, P.V.; and Kitanidis, K.: Prediction of single phase transport parameters in a variable aperture fracture, Geophys. Res. Lett., 22, (1995), 1425-1428

Keller, A.A.; Roberts, P.V.; Blunt, M.J.: Effects of fracture aperture variations on the dispersion of contaminants, Water Resour. Res., 35(1), (1999), 55-63

Konzuk, J.S., and Kueper, B.H.: Evaluation of cubic law based models describing single-phase flow through a rough-walled fracture, Water Resour. Res., 40, (2004), W02402, doi:10.1029/2003WR002356

Liu, J.; Sheng, J.; Polak, A.; Elsworth, D.; Yasuhara, H.; and Geader, A.: A fully-coupled hydrological-mechanical-chemical model for fracture sealing and preferential opening, Int. J. Rock. Mech. Min. Sci., 43, (2006), 23-36

Montemagno, C.D., and Pyrak-Nolte, L. J.: Fracture network versus single fractures: measurement of fracture geometry with X-ray tomography, Phys. Chem. Earth, 24(7), (1999), 575-579

Mourzenko, V.V.; Thovert, J.-F.; and Adler, P. M.: Permeability of a single fracture: Validity of the Reynolds equation, J. Phys. II Fr., 5(3), (1995), 465-482

Nakashima, Y.; Kamiya, S.; and Nakano, T.: Diffusion ellipsoids of anisotropic porous rocks calculated by X-ray computed tomography-based random walk simulations, Water Resour. Res., 44, (2008), W12435, doi: 10.1029/2008WR006853

Nemoto, K.; Watanabe, N.; Hirano, N.; and Tsuchiya, N.: Direct measurement of contact area and stress dependence of anisotropic flow through rock fracture with heterogeneous aperture distribution, Earth Planet. Sci. Lett., 281, (2009), 81-87

Oron, A.P.; and Berkowitz, B.: Flow in rock fractures: The local cubic law assumption reexamined, Water Resour. Res., 34(11), (1998), 2811-2825

Polak A.; Grader, A.S.; Wallach, R.; and Nativ, R.: Chemical diffusion between a fracture and the surrounding matrix: Measurement by computed tomography and modeling, Water Resour. Res., 39(4), (2003), 1106, doi: 10.1029/2001WR000813

Polak, A.; Elsworth, D.; Liu, J.; and Grader, A.S.: Spontaneous switching of permeability changes in a limestone fracture with net dissolution, Water Resour. Res., 40, (2004), W03502, doi: 10.1029/ 2003WR002717

Pyrak-Nolte, L.J., Montemagno, C.D., and Nolte, D.D.: Volumetric imaging of aperture distributions in connected fracture networks, Geophys. Res. Lett., 24(18), (1997), 2343-2346

Pyrak-Nolte, L.J.; and Morris, J.P.: Single fractures under normal stress: The relation between fracture specific stiffness and fluid flow, Int. J. Rock Mech. Min. Sci., 37(1-2), (2000), 245-262

Rangel-German, E.R.; Kovscek, A.R.: Experimental and analytical study of multidimensional imbibition in fractured porous media, J. Petrol. Sci. Eng., 36, (2002), 45-60

Ribeiro, J.L.B; Queiroz, J.C.; Lopes, R.T.; Anjos, M.J.; Bianco, L.C.B.; D'Almedia, A.R.; and Campos, E.F.: New methodology for analysis of performance for diverting agents in unconsolidated sandstones in real time with physical simulator using computed tomography, Nucl. Instrum. Methods Phys. Res. A, 579, (2007), 481-485

Rowland, J.C.; Manga, M.; and Rose, T.P.: The influence of poorly interconnected fault zone flow paths on spring geochemistry, Geofluids, 8, (2008), 93-101, doi:10.1111/j.1468-8123.2008.00208.x

Scavia, F.Re, C.: Determination of contact areas in rock joints by X-ray computed tomography, Int. J. Rock Mech. Min. Sci., 36, (1999), 883-390

Watanabe, N.; Hirano, N.; and Tsuchiya, N.: Determination of aperture structure and fluid flow in a rock fracture by high-resolution numerical modeling on the basis of a flow-through experiment under confining pressure, Water Resour. Res., 44, (2008), W06412, doi: 10.1029/2006WR005411

Watanabe, N.; Hirano, N.; and Tsuchiya, N.: Diversity of channeling flow in heterogeneous aperture distribution inferred from integrated experimental numerical analysis on flow through shear fracture in granite, J. Geophys, Res., 114, (2009), in press

Yasuhara, H.; Polak, A.; Mitani, Y.; Grader, A.S.; Halleck, P.M.; and Elsworth, D.: Evolution of fracture permeability through fluid-rock reaction under hydrothermal conditions, Earth Planet. Sci. Lett., 244, (2006), 186-200

Yeo, I.W.; de Freitas, M.H.; and Zimmerman, R.W.: Effect of shear displacement on the aperture and permeability of a rock fracture, Int. J. Rock Mech. Min. Sci., 35(8), (1998), 1051– 1070.

Zhu, W.C.; Liu, J.; Elsworth, D.; Polak, A.; Grader, A.; Shen, J.C.; and Liu, J.X.: Tracer transport in a fractured chalk: X-ray CT characterization and digital-image-based (DIB) simulation, Transp. Porous Med., 70, (2007), 25-42

Zimmerman, R.W., and Bodvarsson, G. S.: Hydraulic conductivity of rock fractures, Transp. Porous Media, 23, (1996), 1-30